Talanta 111 (2013) 105–110

Contents lists available at SciVerse ScienceDirect

Talanta

journal homepage: www.elsevier.com/locate/talanta

A highly selective sandwich-type FRET assay for ATP detection based on silica coated photon upconverting nanoparticles and split aptamer

Xiaoxiao He, Zhangxiu Li, Xuekun Jia, Kemin Wang*, Jinjin Yin

State Key Laboratory of Chemo/Biosensing and Chemometrics, College of biology, College of Chemistry & Chemical Engineering, Hunan University, Key Laboratory for Bio-Nanotechnology and Molecule Engineering of Hunan Province, Changsha 410082, PR China

ARTICLE INFO

Article history:
Received 12 December 2012
Received in revised form
18 February 2013
Accepted 20 February 2013
Available online 27 February 2013

Keywords:
ATP
Silica coated photon upconverting
$NaYF_4$:Yb^{3+}
Er^{3+} nanoparticles (Si@UCNPs)
Split aptamer
Optical sandwich assay

ABSTRACT

In this paper, we report a highly selective sandwich-type fluorescence resonance energy transfer (FRET) assay for ATP detection by combining the unique optical properties of silica coated photon upconverting $NaYF_4$:Yb^{3+}, Er^{3+} nanoparticles (Si@UCNPs) with the high specific recognition ability of ATP aptamer. In the protocol, a single aptamer of ATP was split into two fragments. One of which was covalently attached to the Si@UCNPs at the 5′ end, and the other was labeled with Black Hole Quencher-1 (BHQ1) at the 3′ end. In the presence of ATP, the two fragments bound ATP with high affinity to form the sandwich complexes on the surface of Si@UCNPs. ATP induced association of the two fragments, thus bringing the Si@UCNPs and BHQ1 into close proximity. Under the illumination of 980 nm laser, energy transfer took place between the Si@UCNPs as the donor and BHQ1 as the acceptor, creating an optical "sandwich-type" assay for ATP detection. By monitoring the fluorescence change of the Si@UCNPs at 550 nm, the presence of the ATP could be quantitatively detected with a detection limit of 1.70 μM. The linear response range was 2 μM–16 μM. The background of this assay was ignorable because the fluorescence intensity of Si@UCNPs at 550 nm was not changed in the absence of ATP. This assay was also able to discriminate ATP from its analogs.

1. Introduction

Adenosine-5′-triphosphate (ATP), a multifunctional nucleoside, is most important as a 'molecular currency' of intracellular energy transfer in all living cells [1]. It is an energy source produced during photosynthesis and cellular respiration and could be consumed by many enzymes for all the biological processes, including metabolism of foods, synthesis of biologically important molecules, transportion of molecules and ions, contraction of muscle, and other cellular movements [2]. ATP itself also serves as an intra- and extracellular signaling molecule. For instance, extracellular ATP acts as a signaling molecule that regulates a variety of cellular responses through binding to specific G protein coupling receptors-P2 purinoceptors [3]. Apart from its roles in energy metabolism and signaling, ATP is also incorporated into nucleic acids by polymerases in the processes of DNA replication and transcription [4]. In addition, the amount of ATP can reflect the level of microbial contamination in food, water, medicine and makeup [5]. Therefore, it is of high importance to develop assay toward ATP detection with high selectivity for life science study, clinical medical research as well as food quality control and environmental monitoring. Antibody-based immunoassay system and ATP-dependent enzymatic reaction system are the two of the most selective and powerful tools for ATP analyses in research [6,7], medical diagnostics [8–10], and environmental monitoring [11,12]. However, shortcomings with the production, stability, and cost of the antibody and bioluminescence reagents limit their extensively application.

Aptamers are single-stranded DNA or RNA sequences which possess high recognition ability to specific targets ranging from small inorganic, organic substances, proteins, to even intact viruses or tumor cells and form defined tertiary structures upon specific targets binding [13,14]. They are artificially selected from random-sequence nucleic acids libraries through systematic evolution of ligands by exponential enrichment (SELEX). Aptamers can rival traditional recognition elements for molecular recognition and detection due to their good stability, simple synthesis, easy labeling, wide applicability, high resistance against denaturation, and high sensitivity [15]. In addition, the other important feature of the aptamers is the conformation change resulting from its specific binding to targets, which lead to develop various aptamers based sensing system for the targets detection with high sensitivity and selectivity, including optical transduction [16], fluorescence [17], colorimetry [18], electrochemistry [19,20], and so on. For the ATP detection, one of the most elegant aptamer-based sensing systems is the fluorescent method which

* Corresponding author. Tel./fax: +86 731 88821566.
E-mail address: kmwang@hnu.edu.cn (K. Wang).

0039-9140/$ - see front matter © 2013 Elsevier B.V. All rights reserved.
http://dx.doi.org/10.1016/j.talanta.2013.02.050

is operated on the structure switching/fluorescence-dequenching mechanism [21–23]. As references reported, there are mainly two kinds of strategies to perform structure switching/fluorescence-dequenching. One of the strategies makes use of a fluorophore-labeled ATP aptamer [24,25]. When a quencher-labeled complementary DNA is hybridized with the fluorophore-labeled ATP aptamer to form duplex DNA, the fluorescence quenching is taken place due to the close proximity of the fluorophore and the quencher. The presence of the ATP would switch the duplex to an aptamer–ATP complex, resulting in dequenching of the fluorophore and an increase in the fluorescence signal. The other strategy is based on the split aptamers [26]. The single aptamer of ATP is split into two fragments which are labeled using fluorophore and quencher, respectively. The formation of a folded, associated complex upon binding with ATP will operate the fluorescence–quencher distance change. For both of the strategies, organic fluorophores [27,28] and semiconductor quantum dots (QDs) [29,30] are used to label the ATP aptamer or its complementary DNA for signaling the detection of ATP. By compared with organic fluorophores [31], QDs [32] displayed the virtues of higher fluorescence quantum yields, narrower emission bands but higher Stokes shifts, and stability against photobleaching. However, the excitation of the QDs usually requires the use of ultraviolet (UV) or visible radiation. Therefore, the detection backgrounds in actual biological and environmental samples may be substantially enhanced due to the significant autofluorescence came from the interfering biomolecules, such as and nucleic acids and protein under UV rays exaction.

Upconversion nanoparticles (UCNPs) are excited by lower energy photons, usually near-infrared (NIR), but emitted higher energy light (visible) through sequential absorption of multiplephotons or energy transfers [33,34]. Excitation in the NIR induces only a very weak autofluorescence background. Consequently, UCNPs have become one of the most promising classes of luminescent materials for bioanalysis and bioimaging [35,36]. In this work, the UCNPs based split aptamer fluorescence sensing system for ATP detection has been developed by using the structure switching/fluorescence-dequenching mechanism. Herein, 27-base anti-ATP aptamer was employed and split into two fragments. One was labeled with amino group at the 5′ end for conjugation with UCNPs. The other was labeled with Black Hole Quencher-1 (BHQ1) at the 3′ end. To improve the hydrophilicity and facilitate the aptamer fragment immobilization, silica coating was introduced on the surface of the prepared upconverting $NaYF_4$:Yb^{3+}, Er^{3+} nanoparticles, denoted as Si@UCNPs. Owing to the formation of associated complexes upon binding ATP, the distance between Si@UCNPs and BHQ1decreased and fluorescence resonance energy transfer (FRET) therefore took place. The green upconversion fluorescence of Si@UCNPs at 550 nm was decreased by the quench of BHQ1. Thus, a highly selective sandwich-type FRET assay for ATP detection based on Si@UCNPs and split aptamer has been constructed.

2. Experimental section

2.1. Materials and instruments

Adenosine 5-triphosphate (ATP), cytosine 5-triphosphate (CTP), guanosine 5-triphosphate (GTP), and uridine 5-triphosphate (UTP), 1-ethyl-3-(3-dimethylaminopropyl) carbodiimide hydrochloride (EDC), N-hydroxysulfosuccinimide sodium salt (sulfo-NHS), Yttrium chloride hexahydrate ($YCl_3 \cdot 6H_2O$), Ytterbium chloride hexahydrate ($YbCl_3 \cdot 6H_2O$), Erbium chloride hexahydrate ($ErCl_3 \cdot 6H_2O$) (purity > 99.9%) were all obtained from Sigma-Aldrich. N-[(3-trimethoxysilyl)-propyl]ethylenediamine triacetic acid (TMS–EDTA) was purchased from Gelest, Inc and used as received. All the other chemicals were purchased from Reagent & Glass Apparatus Corporation of Changsha and were used without further purification. Deionized water (DI water, Milli-Q 18.2 MΩ cm, Millipore System Inc.) was used in the preparation of all aqueous solutions. The split ATP aptamers were obtained by Sangon Biotechnology Inc. (Shanghai, China). The sequences are as follows: Aptamer 1 (Apt1): 5′-NH_2C_6-T6ACCTGGGGGAGTAT-3′; Aptamer 2 (Apt2): 5′-TGCGGAGGAAGGT-BHQ1-3′.

The ED53 oven was used as the heat supporting equipment. High-resolution transmission electron microscopy (HRTEM) images of $NaYF_4$:Yb^{3+}, Er^{3+} UCNPs and Si@UCNPs were obtained from a JEOL 3010 microscope with accelerating voltage of 200 kV. All fluorescence spectra were recorded on a Hitachi F-4500 FL spectrophotometer with an external 0–1.3 W adjustable laser (980 nm, Beijing Hi-Tech Optoelectronic Co., China) as the excitation source. Malvern Zetasizer Nano ZS was used to perform the zeta potential measurements in an automatic mode. All experiments were done at 25 °C.

2.2. Synthesis of oleic acid-capped $NaYF_4$:Yb^{3+}, Er^{3+} UCNPs.

The $NaYF_4$:Yb^{3+}, Er^{3+} UCNPs were synthesized by a modified hydrothermal process [37]. Briefly, NaOH (1 g, 24.4 mmol), water (5 mL), ethanol (8.5 mL) and oleic acid (17 mL) were mixed to form a homogeneous solution. Subsequently, 0.6 mmol (total amounts) of rare-earth chloride (1.2 mL, 0.5 mol/L $LnCl_3$, Ln: 78 mol%Y+20 mol%Yb+2 mol%Er) aqueous solution was added slowly under magnetic stirring, and then blended adequately 10 min to form a homogeneous solution. The solution of 1.0 mol/L aqueous NaF (4 mL) was slowly added to the above solution later on. The mixture was stirred for about 10 min, then slowly added into a 50 mL autoclave, obturated, and hydrothermally treated at 120 °C for 30 min, then heated to 200 °C for 8 h. After the solution was cooled to room-temperature naturally, cyclohexane (3 mL) was used to dissolve and collect the $NaYF_4$:Yb^{3+}, Er^{3+} UCNPs with oleic acid coating (oleic acid-capped $NaYF_4$:Yb^{3+}, Er^{3+} UCNPs). The products were subsequently deposited by adding ethanol (10 mL) to the sample-containing cyclohexane solution. The resulting mixture was then centrifuged to obtain powder samples. Then the precipitate samples were purified by washing three times with ethanol. Finally, the samples was scattered and kept in cyclohexane (10 mL) for the next experiment operation.

2.3. Preparation and modification of Si@UCNPs.

A typical Stöber-based method was used to modify the surface of oleic acid-capped $NaYF_4$:Yb^{3+}, Er^{3+} UCNPs. Typically, the 50 mg of oleic acid-capped $NaYF_4$:Yb^{3+}, Er^{3+} UCNPs was dispersed in 60 mL of cyclohexane by sonication and agitation for 90 min, and then 6 mL of tertiary butyl alcohol and 10.8 mL of Trion-X 100 were added and mixed by sonication for 10 min. Thereafter, 0.3 mL of ammonia (wt. 28%) was added into the mixture and sonicated for 20 min until a transparent emulsion was formed. 2 μL of tetraethoxysilane (TEOS) was then added into the solution to form silica coated $NaYF_4$:Yb^{3+}, Er^{3+} UCNPs (Si@UCNPs). After stirring for 24 h at a speed of 800 rpm, 6 μL of TMS–EDTA was added and stirred for further 24 h to modify the Si@UCNPs with carboxyl group. The carboxyl modified Si@UCNPs were then collected by adding ethanol demulsification and centrifugation. Finally, the carboxyl modified Si@UCNPs were washed several times with ethanol and water, and then dried in vacuum at 60 °C for 12 h.

2.4. Attachment of aptamer onto the carboxyl modified Si@UCNPs.

The attachment of the aptamer onto the carboxyl modified Si@UCNPs was carried out via EDC/NHS crosslinking method. Briefly, 8 mg of EDC and 16 mg of sulfo-NHS were added to 1 mL of 0.1 M MES buffer (pH 6.0) containing 8 mg of carboxyl modified Si@UCNPs. The mixture was placed in the table concentrator and stirred at the speed of 350 rpm for 30 min at room temperature. The precipitate was obtained by centrifugation and washed with sterile water, and then was added into 1 mL of 2 μM Apt 1 solution (pH 8.0). The mixed suspension was set in the table concentrator and stirred at the speed of 350 rpm over night at room temperature. Finally, Apt 1 functionalized Si@UCNPs (Apt1-Si@UCNPs) were received by centrifugation, and washed several times with sterile water.

2.5. Fluorescent detection of ATP

For the detection of ATP, a complex solution consisted with Apt1-Si@UCNPs (2 mg/mL) and Apt2 (90 nM) was taken into a cuvette after sonicating the stock solution to ensure homogenous suspension of nanoparticles in 100 mM Tris–HCl buffer (2 mM $MgCl_2$, pH 8.0). The complex solution was treated as blank, and photoluminescence spectrum was taken under the exaction of 980 nm. Subsequently, an increment of 2 μL ATP with different concentration was then added to the blank. Before taking spectra, there was a 30 min incubation under stirring at 25 °C to allow for complete recognition and binding reaction. For control experiment, 2 μL of 100 mM Tris–HCl buffer was added and the photoluminescence spectrum was taken.

3. Results and discussion

3.1. Detection principle.

The schematic diagram of this fluorescent sandwich assay for ATP detection using Si@UCNPs and split aptamer is shown in Fig. 1. The principle for fluorescent detecting ATP was based on the FRET model in which donor and acceptor are brought into FRET proximity through specific recognition of the ATP aptamer. Herein, the aptamer of ATP was split into two fragments. The Si@UCNPs were used as the energy donor and covalently modified with one of the aptamer fragments (Apt1). The other aptamer fragment (Apt2) was labeled with BHQ1 which used was as energy acceptor in this assay. In the absence of ATP, obvious emission wavelength of the Si@UCNPs appear around 550 and 650 nm upon excitation by an infrared (~980 nm) laser. The 550 nm emission matches well with the absorption of BHQ1 (480–580 nm), used as the fluorescence quencher in this work. In the presence of ATP, the known selective recognition and binding of the two split aptamer fragments with ATP induced the formation of sandwich complexes and brought Si@UCNPs and BHQ1 into appropriate proximity and hence induced energy transfer. Thereafter, energy transfer from Si@UCNPs to BHQ1 was then investigated by measuring the fluorescence quenching rate ($Q_r=(Fo_{550\ nm}-F_{550\ nm})/Fo_{550\ nm}$) of Si@UCNPs at emission of 550 nm, where $Fo_{550\ nm}$ was the fluorescence intensity of Si@UCNPs at emission of 550 nm before ATP addition, and $F_{550\ nm}$ was the fluorescence intensity of Si@UCNPs at emission of 550 nm after ATP addition. The fluorescence quenching rate then could reflect the concentration of ATP.

3.2. Characterization of oleic acid-capped UCNPs and Si@UCNPs

Fig. 2a shows the TEM image of oleic acid-capped UCNPs. It can be seen that the as-prepared oleic acid-capped $NaYF_4$:Yb^{3+}, Er^{3+} UCNPs were cubic phase in shape. Due to the capping of oleic acid on their surface of $NaYF_4$:Yb^{3+}, Er^{3+} UCNPs, they were not water-soluble and then surface modification was necessary before their use in the subsequent biological detections. In our work, the $NaYF_4$:Yb^{3+}, Er^{3+} UCNPs were first coated by a silica shell and further functionalized with TMS–EDTA to form carboxyl modified Si@UCNPs via a typical Stöber-based modification method. As shown in the Fig. 2b, it can be obviously observed that the as-prepared carboxyl modified Si@UCNPs were coated with a layer of silica and still appeared cubic in shape (see the arrows in Fig. 2b). The thickness of the silica layer could be controlled between 2.5–1.5 nm. To further verify the surface carboxyl modification of $NaYF_4$:Yb^{3+}, Er^{3+} UCNPs, the zeta potential of oleic acid-capped $NaYF_4$:Yb^{3+}, Er^{3+} UCNPs before and after modification were analyzed by using Malvern Zetasizer Nano ZS. The zeta potential of the acid-capped $NaYF_4$:Yb^{3+}, Er^{3+} UCNPs was −31.0 mV. After modification, the zeta potential of

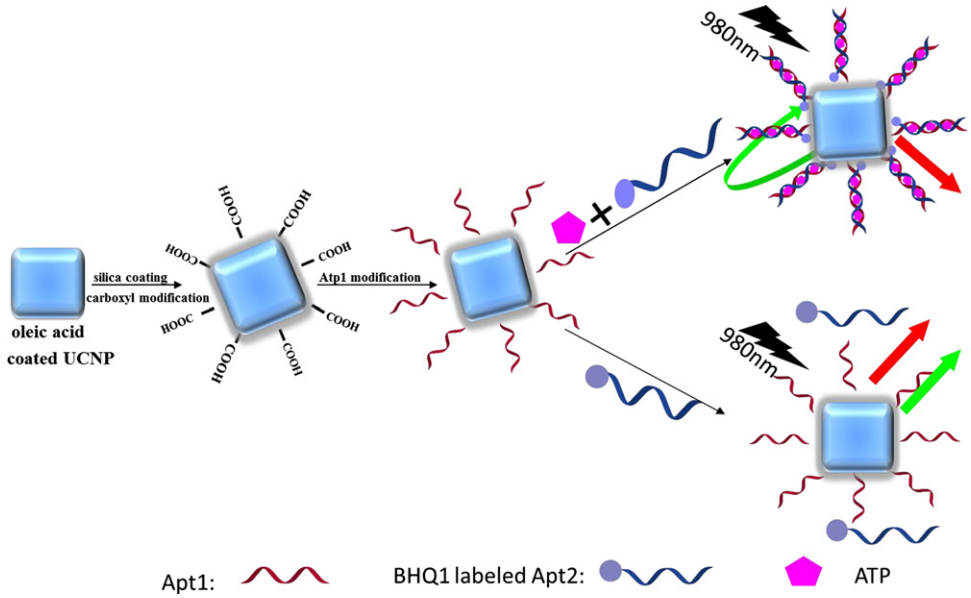

Fig. 1. The schematic representation of the sandwich-type FRET assay for ATP detection based on silica coated photon upconverting nanoparticles and split aptamer.

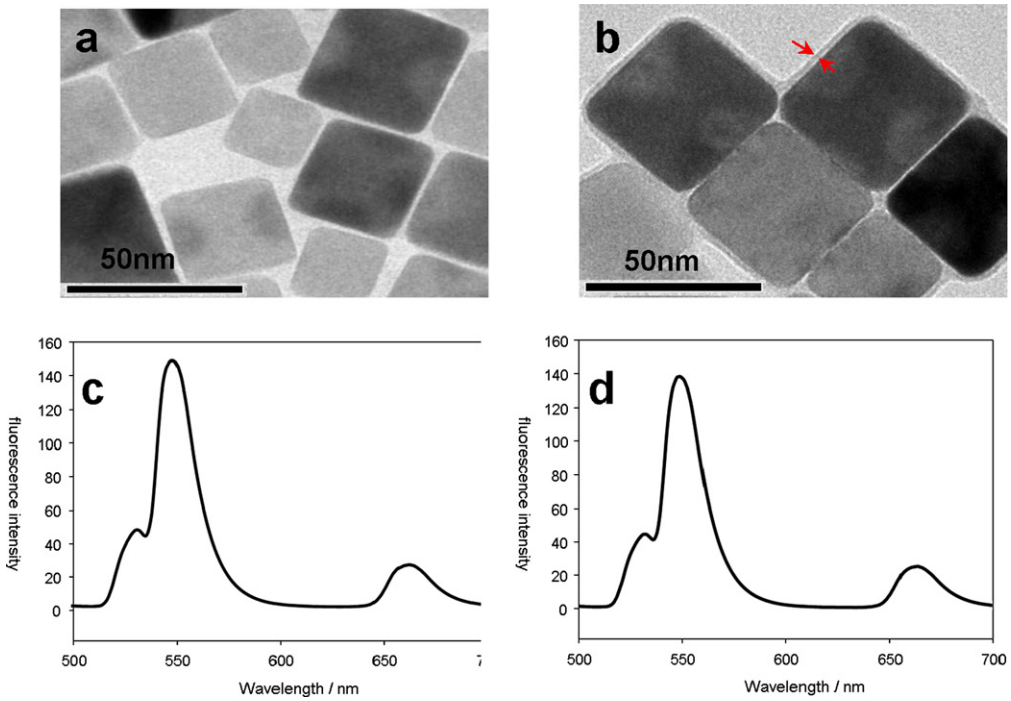

Fig. 2. TEM images and fluorescence spectrum (λex=980 nm) of oleic acid-capped $NaYF_4$:Yb^{3+}, Er^{3+} UCNPs before (a, c) and after silica coating (b, d). Ex: 980 nm. (For interpretation of the references to color in this figure, the reader is referred to the web version of this article.)

carboxyl modified Si@UCNPs was about −47.1 mV, suggesting the carboxyl modified Si@UCNPs was successful formed. After coating with silica shell, the resultant carboxyl modified Si@UCNPs were not only dispersible in water with good chemical and photochemical stability but also possessed the carboxyl groups on the surface.

The photoluminescence spectra of the oleic acid-capped $NaYF_4$:Yb^{3+}, Er^{3+} UCNPs and carboxyl modified Si@UCNPs is shown in Fig. 2c and d. For the oleic acid-capped $NaYF_4$:Yb^{3+}, Er^{3+} UCNPs, two emission bands are found in the spectrum: a green emission at 550 nm and a red emission at 650 nm. After silica modification, fluorescent intensity and photoluminescence spectrum of the as-prepared Si@UCNPs did not change. We can see that the red emission at 650 nm is very weak compared to the green emission at 550 nm for both of the oleic acid-capped $NaYF_4$:Yb^{3+}, Er^{3+} UCNPs and carboxyl modified Si@UCNPs. Therefore, the $NaYF_4$:Yb^{3+}, Er^{3+} UCNPs with the strong green emission were just suitable for use as an energy donor for BHQ1 in the FRET assay.

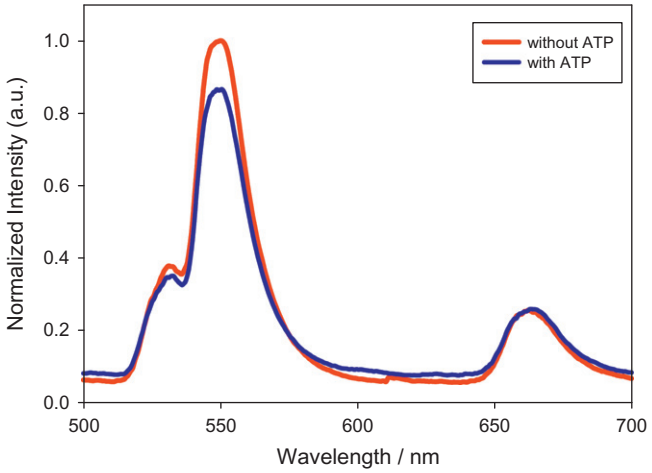

Fig. 3. The fluorescence spectrum of the mixture of Apt1 modified Si@UCNPs and Apt2 in different systems. (Ex: 980 nm). (For interpretation of the references to color in this figure, the reader is referred to the web version of this article.)

3.3. *Feasibility investigation of the assay.*

After the Apt1 was modified onto the surface of carboxyl modified Si@UCNPs via EDC/NHS crosslinking method, a fluorescence measurement was then used to explore the feasibility of the assay for ATP detection. As shown in Fig. 3, when 2 μL of 1.0 mM ATP was added into the mixture of 2 mg/mL Apt1 modified Si@UCNPs and Apt2 with a 1.5:1 M ratio of Apt1 to Apt2 (in 0.1 m Tris–HCl buffer, pH 8.0, 2 mg mL^{-1} Mg^{2+}), the green emission at 550 nm was quenched obviously, whereas the red emission at 650 nm remained almost unchanged. However, both of the green emission and red emission of Apt1 modified Si@UCNPs was not changed if ATP was not added. The results suggested that the sandwich complex on the surface of Si@UCNPs could form in the presence of ATP, thus bringing the Si@UCNPs and BHQ1 into close proximity and energy transfer from Si@UCNPs to BHQ1 was produced. Therefore, the Si@UCNPs and split aptamer based fluorescent sandwich assay could be used for ATP detection.

3.4. *Optimization of assay conditions*

3.4.1. *Effect of concentration of Si@UCNPs*

The Si@UCNPs is the key part in this fluorescent assay, which not only was the fluorescence donor but also acted as the carriers for Apt1 attachment. The concentration of Si@UCNPs was firstly optimized in this experiment. It was demonstrated that the fluorescence quenching rate of green emission at 550 nm was increased by changing the concentration of Si@UCNPs from 0 mg/mL to 2 mg/mL (Fig. 4a). The quenching rate tended to decrease when the concentration of Si@UCNPs was up to 2 mg/mL. Therefore, 2 mg/mL Si@UCNPs was chosen for the following experiments.

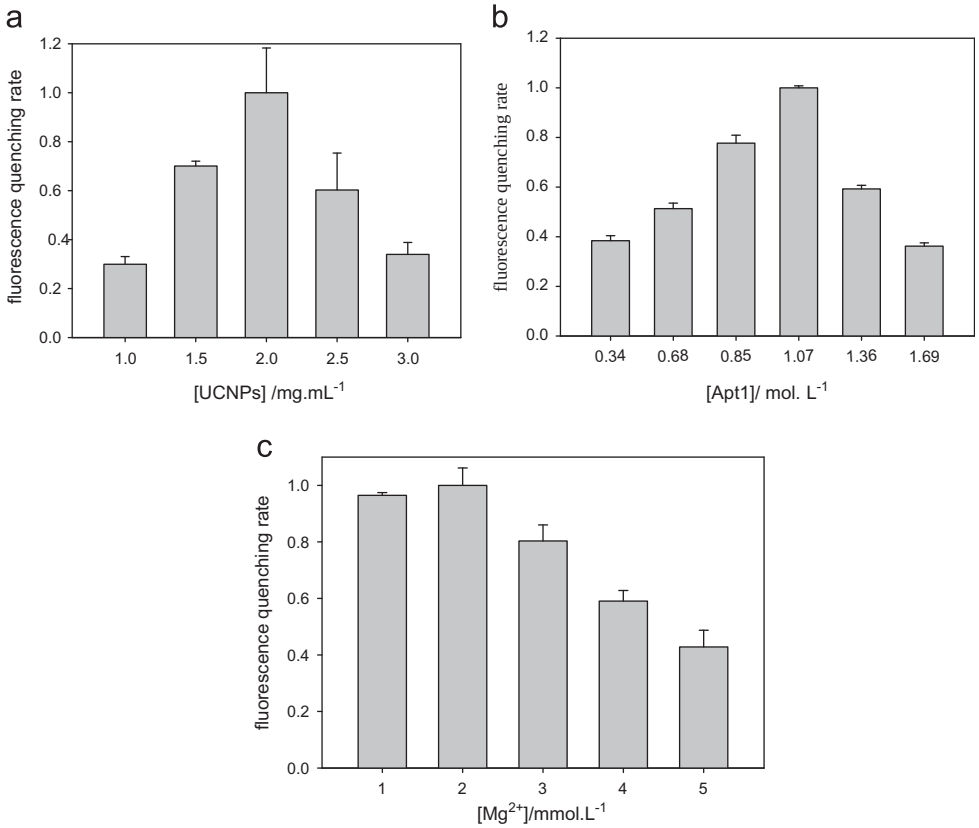

Fig. 4. Optimization of experimental conditions (incubation time: 30 min, 25 °C). (a) Effect of concentration of Si@UCNPs. (b) Effect of different modification concentration of Apt1. (c) Effect of Mg^{2+} concentration.

3.4.2. *Effect of different modification concentration of Apt1*

The modification concentration of Apt1 was also optimized in this experiment. Fig. 4b showed that the fluorescence quenching rate was increased by varying the Apt1 concentration from 0.34 to 1.07 μM. When the concentration of Apt1 exceeded 1.07 μM, the fluorescence quench efficiency tended to decrease. Thus, 1.07 μM of Apt1 was selected for the following experiments.

3.4.3. *Effect of Mg^{2+} concentration*

It is known the Mg^{2+} concentration may affect the affinity of an aptamer to its target molecule. Therefore, the effect of Mg^{2+} concentration (from 1 mmol/L to 5 mmol/L) on this assay system has been investigated. As shown in Fig. 4c, the fluorescence quenching rate was the highest when the Mg^{2+} concentration was 2 mmol/L.

3.5. *ATP detection*

Under the optimal conditions, a series of ATP solutions with final concentration from 1 to 50.0 μM were detected by employing the sandwich-type FRET system consisting of the Apt1-conjugated Si@UCNPs (donor) and BHQ1 labeled Apt2 (acceptor). Fig. 5 showed the response curve, where fluorescence quenching rate ($Fo_{550\ nm}-F_{550\ nm}$)/$Fo_{550\ nm}$ was plotted against the ATP concentration. It was demonstrated the fluorescence quenching rate ($Fo_{550\ nm}-F_{550\ nm}$)/$Fo_{550\ nm}$ was increased gradually with the increasing amount of ATP in the concentration from 1 to 20.0 μM, suggesting that the efficiency of energy transfer from green emission to the acceptor was increased. When the concentration of ATP was further increased, the fluorescence quenching rate ($Fo_{550\ nm}-F_{550\ nm}$)/$Fo_{550\ nm}$ remained nearly constant. The reason was that the formation of sandwich complex in the FRET system was saturated at a higher concentration of ATP.

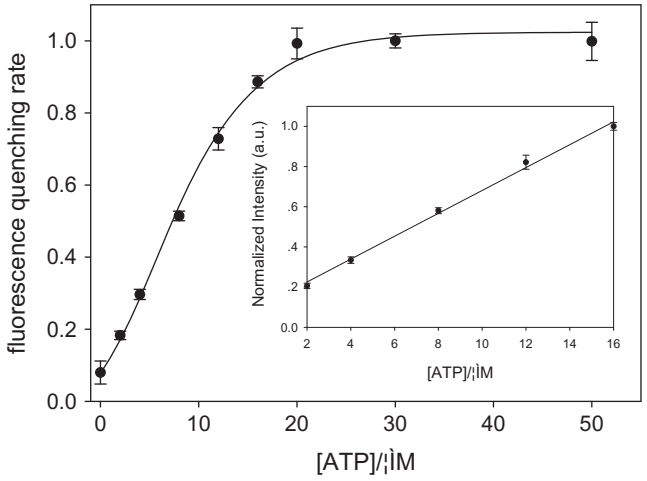

Fig. 5. The fluorescence quenching rates of the sandwich-type FRET system at different concentrations of ATP (0, 10, 20, 30, 40, 50 uM) in 0.1 M Tris–HCl buffer (pH 8.0, 2 mg mL^{-1} Mg^{2+}). Inset: the linear relationship between the fluorescence recovery and the concentration of ATP within the range of 2–15 μM.

The linear relationship between the fluorescence quenching rate ($Fo_{550\ nm}-F_{550\ nm}$)/$Fo_{550\ nm}$ and ATP concentration was over the range of 2–16 μM with a correlation factor 0.997. The linear regression equation was $y=0.058x+0.0995$ (here, x was the concentration of ATP (μM), and y was the fluorescence quenching rate). The detection limit was 1.70 μM calculated according to the signal/noise of 3. It is worthwhile to point out that the green emission at 550 nm is quenched remarkably in the presence of ATP, whereas the red emission at 650 nm remains almost unchanged. Therefore, the emission at 650 nm could be used as an internal standard reference.

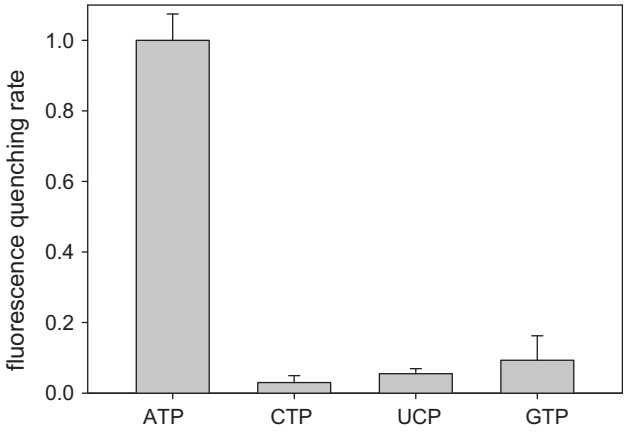

Fig. 6. The fluorescence quenching rates of the sandwich-type FRET system incubated with ATP, CTP, UCP and GTP, respectively in 0.1 M Tris–HCl buffer (pH 8.0, 2 mg mL^{-1} Mg^{2+}).

We also reviewed the fluorescence intensity ratio between the emission at 550 nm to 650 nm of the Si@UCNPs by excited with 980 nm laser ($F_{550\ nm}/F_{650\ nm}$). Between the fluorescence decrease ($F_{550\ nm}/F_{650\ nm}$) and the concentration of ATP, there was also a good linear relationship within range of ~2–16 μM with a correlation coefficient of 0.997.

In this work, the selectivity of this sandwich-type FRET system for ATP detection has also been tested by comparing the fluorescence quenching rate of sandwich-type FRET system containing ATP and the three other analogs, including CTP, UTP, and GTP, which belong to the nucleoside triphosphate family. The fluorescence quenching rate was investigated individually after ATP, UTP, CTP, and GTP with the same concentration of 20 nM were added respectively. The experimental results were shown in Fig. 6. It was demonstrated that the fluorescence quenching rate was ignorable after the addition of UTP, CTP, or GTP at the concentration of 20 nM, but it does show significant fluorescence quenching after the addition ATP. This result obviously indicated that the proposed the sandwich-type FRET system consisting of the Apt1-conjugated Si@UCNPs (donor) and BHQ1 labeled Apt2 had sufficient selectivity in ATP detection, and was able to discriminate ATP from its analogs.

4. Conclusions

In the present study, a highly selective sandwich-type FRET assay for ATP detection has been developed based on silica coated photon upconverting nanoparticles and split aptamer. In this assay, a single aptamer of ATP was split into two fragments. Silica coated photon upconverting nanoparticles (Si@UCNPs) were used as donor and carriers for immobilizing one of the aptamer fragments (Apt1). Black Hole Quencher-1 (BHQ1) labeled on the other aptamer fragment (Apt2) was acted as acceptor. A sandwich-type FRET system between the Apt1 modified Si@UCNPs and BHQ1 labeled Apt2 was formed in the presence of ATP due to the high affinity binding of ATP with the two aptamer fragments, which make the distance between the donors and the acceptors short enough for FRET to occur. By using this sandwich-type FRET system, we can quantitatively detect the presence of ATP with a detection limit of 1.70 μM. In addition, the sandwich-type FRET system offered very high selectivity in discriminating ATP from the three ATP analogs. It is expected that the sandwich-type FRET system provides a useful model for the detection of other kind of biomolecules when the Si@UCNPs and acceptor are modified by proper molecules that can recognize the target biomolecules.

Acknowledgment

This work was supported in part by the Project of Natural Science Foundation of China (21175039 and 21190044), Key Technologies Research and Development Program of China (2011AA02a114), Research Fund for the Doctoral Program of Higher Education of China (20110161110016) and Project supported by Hunan Provincial Natural Science Foundation and Hunan Provincial Science and Technology Plan of China (10JJ7002, 2012TT1003).

References

[1] T. Tatsumi, J. Shiraishi, N. Keira, K. Akashi, A. Mano, S. Yamanaka, S. Matoba, S. Fushiki, H. Fliss, M. Nakagawa, Cardiovasc. Res. 59 (2003) 428–440.
[2] S.H. Larsen, J. Adler, J.J. Gargus, R.W. Hogg, PNAS 71 (1974) 1239–1243.
[3] L. Xie, M. Zhang, W. Zhou, Z.-G. Wu, J.-G. Ding, L.-Y. Chen, T. Xu, Traffic 7 (2006) 429–439.
[4] S. Bell, B. Stillman, Nature 375 (1992) 128–134.
[5] J.-P. Luo, X.-H. Liu, Q. Tian, W.-W. Yue, J. Zeng, G.-Q. Chen, X.-X. Cai, Anal. Biochem. 394 (2009) 1–6.
[6] R. Sprung, R. Sprague, D. Spence, Anal. Chem. 74 (2002) 2274–2278.
[7] P. Mahato, A. Ghosh, S.K. Mishra, A. Shrivastav, S. Mishra, A. Das, Chem. Commun. 46 (2010) 9134–9136.
[8] E. Llaudet, S. Hatz, M. Droniou, N. Dale, Anal. Chem. 77 (2005) 3267–3273.
[9] J.-F. Masson, C. Kranz, B. Mizaikoff, E.B. Gauda, Anal. Chem. 80 (2006) 3991–3998.
[10] C.-B. Ma, H.-C. Chen, R. Han, H.-L. He, W.-M. Zeng, Anal. Biochem. 429 (2012) 8–10.
[11] N.-C. Yang, W.-M. Ho, Y.-H. Chen, M.-L. Hu, Anal. Biochem. 306 (2002) 323–327.
[12] K. Venkateswaran, N. Hattori, M.T.L. Duc, R. Kern, J. Microbiol. Methods 52 (2003) 367–377.
[13] G.-T. Song, C.-E. Chen, X.-G. Qu, Adv. Mater. 20 (2008) 706–710.
[14] A.-P. Xin, Q.-P. Dong, C. Xiong, L.-S. Ling, Chem. Commun. 13 (2009) 1658–1660.
[15] K.-M. Song, S. Lee, C. Ban, Sensors 12 (2012) 612–631.
[16] J. Zhang, L.-H. Wang, H. Zhang, F.Y. Boey, S.-P. Song, C.-H. Fan, Small 6 (2010) 201–204.
[17] X.-D. Zeng, X.-L. Zhang, W. Yang, H.-Y. Jia, Y.-M. Li, Anal. Biochem. 424 (2012) 8–11.
[18] Y.-F. Huang, H.-T. Chang, Anal. Chem. 79 (2007) 4852–4859.
[19] X.-L. Zuo, S.-P. Song, J. Zhang, D. Pan, L.-H. Wang, C.-H. Fan, J. Am. Chem. Soc. 129 (2007) 1042–1043.
[20] Y.-H. Wang, X.-X. He, K.-M. Wang, X.-Q. Ni, Biosens. Bioelectron. 25 (2010) 2101–2106.
[21] M.N. Stojanovic, P. Prada, D.W. Landry, J. Am. Chem. Soc. 122 (2000) 11547–11548.
[22] J. Wang, Y.-X. Jiang, C.-S. Zhou, X.-H. Fang, Anal. Chem. 77 (2005) 3542–3546.
[23] J.-S. Zhen, L.-Q. Chen, S.J. Xiao, Y.-F. Li, P.-P. Hu, L. Zhan, L. Peng, E.-Q. Song, C.-Z. Huang, Anal. Chem. 82 (2010) 8432–8437.
[24] R. Nutiu, Y.-F. Li, J. Am. Chem. Soc. 125 (2003) 4771–4778.
[25] Y. He, Z.-G. Wang, H.-W. Tang, D.-W. Pang, Biosens. Bioelectron. 29 (2011) 76–81.
[26] X.-L. Zuo, Y. Xiao, K.W. Plaxco, J. Am. Chem. Soc. 131 (2009) 6944–6945.
[27] L.-W. Yan, Z.-B. Ye, C.-X. Peng, S.-H. Zhang, Tetrahedron Lett. 68 (2012) 2725–2727.
[28] L. Cai, Z.-Z. Chen, X.-M. Dong, H.-W. Tang, D.-W. Pang, Biosens. Bioelectron. 29 (2011) 46–52.
[29] Z. Chen, G. Li, L. Zhang, J.-F. Liang, Z. Li, Z.-H. Peng, L. Deng, Anal. Bioanal. Chem. 392 (2008) 1185–1188.
[30] H.-P. Huang, Y.-L. Tan, J.-J. Shi, G.-X. Liang, J.-J. Zhu, Nanoscale 2 (2010) 606–612.
[31] F. Wang, W.-B. Tan, Y. Zhang, X.-P. Fan, M.-Q. Wang, Nanotechnology 17 (2006) R1–R13.
[32] D.R. Larson, W.R. Zipfel, R.M. Williams, S.W. Clark, M.P. Bruchez, F.W. Wise, W.W. Webb, Science 300 (2003) 1434–1437.
[33] L.-Y. Wang, R.-X. Yan, Z.-Y. Huo, L. Wang, J.-G. Zeng, J. Bao, X. Wang, Q. Peng, Y.-D. Li, Angew. Chem. Int. Ed. 44 (2005) 6054–6057.
[34] X.-X. He, J.-H. Gao, S.S. Gambhir, Z. Cheng, Trends Mol. Med. 16 (2010) 574–583.
[35] J.-L. Liu, Y. Liu, Q. Liu, C.-Y. Li, L.-N. Sun, F.-Y. Li, J. Am. Chem. Soc. 133 (2011) 15276–15279.
[36] Y.-H. Wang, L. Bao, Z.-H. Liu, D.-W. Pang, Anal. Chem. 83 (2011) 8130–8137.
[37] Z.-G. Chen, H.-L. Chen, H. Hu, M.-X. Yu, F.-Y. Li, Q. Zhang, Z.-G. Zhou, T. Yi, C.-H. Huang, J. Am. Chem. Soc. 130 (2008) 3023–3029.